

## Stochastic simulation of destruction processes in self-irradiated materials\*

T. Patsahan<sup>1</sup>, A. Taleb<sup>2,3</sup>, J. Stafiej<sup>4</sup>, M. Holovko<sup>1</sup>, J.P. Badiali<sup>1,3</sup>

<sup>1</sup> Institute for Condensed Matter Physics of the National Academy of Sciences of Ukraine,  
1 Svientsitskii St., 79011 Lviv, Ukraine

<sup>2</sup> PSL Research University, Chimie ParisTech — CNRS, Institut de Recherche de Chimie Paris, Paris 75005, France

<sup>3</sup> Université Pierre et Marie Curie, Paris, 75231, France

<sup>4</sup> Cardinal Stefan Wyszyński University, Department of Mathematics and Natural Sciences, Warsaw, Poland

Received June 19, 2017, in final form August 6, 2017

Self-irradiation damages resulting from fission processes are common phenomena observed in nuclear fuel containing (NFC) materials. Numerous  $\alpha$ -decays lead to local structure transformations in NFC materials. The damages appearing due to the impacts of heavy nuclear recoils in the subsurface layer can cause detachments of material particles. Such a behaviour is similar to sputtering processes observed during a bombardment of the material surface by a flux of energetic particles. However, in the NFC material, the impacts are initiated from the bulk. In this work we propose a two-dimensional mesoscopic model to perform a stochastic simulation of the destruction processes occurring in a subsurface region of NFC material. We describe the erosion of the material surface, the evolution of its roughness and predict the detachment of the material particles. Size distributions of the emitted particles are obtained in this study. The simulation results of the model are in a qualitative agreement with the size histogram of particles produced from the material containing lava-like fuel formed during the Chernobyl nuclear power plant disaster.

**Key words:** nuclear fuel containing material, self-irradiation damage, destruction, roughness, stochastic computer simulation, sputtering

**PACS:** 02.50.-r, 23.70.+j, 05.50.+q, 46.50.+a, 46.65.+g

### 1. Introduction

A study of nuclear fuel containing (NFC) materials and problems related to their storage are of a special interest due to the great importance with respect to the safety of environment. The nuclear waste materials encapsulating actinides (e.g., U, Pu) undergo self-irradiation during long periods of time. Therefore, their chemical and physical properties change crucially. Permanent  $\alpha$ -decay events occurring in a material lead to transformations of material structure around the points where these events appear, producing the so-called thermal spikes [1–4]. Such local structural changes damage a material and can lead to its destruction if the relaxation time related to healing processes is too slow. In homogeneous NFC materials where nuclear fuel is distributed randomly, the damages also appear randomly in the material bulk producing local defects [3]. On the other hand, if these defects occur deep in the bulk they can be healed with time [3, 4], while the defects produced near the material surface can erode this surface which leads to a detachment of the particles formed by material pieces. As a consequence, a highly radioactive surface may spontaneously disseminate and disperse a solid state phase into the environment. In connection with these phenomena, long term predictions are required. However, predictions cannot result from simplified extrapolations of the experimental data measured in limited time scales, which are

\*We dedicate this article to the memory of late Dr. Jean-Pierre Badiali who inspired our research and made a significant contribution to this work.

much shorter than the storage period of the nuclear waste. Therefore, theoretical description appears to be an unavoidable complement to experimental data, and computer simulations become helpful in this case.

There is a large literature describing the damage processes inside nuclear waste materials [5–25]. Self-destruction mechanisms of pure nuclear fuel are also studied. Usually, they try to predict the conditions under which a material bulk becomes unstable (fragile). In most theoretical studies, an atomistic level of modelling is used. For instance, in [8] a method of molecular dynamics is used to simulate the damage processes in zirconolite structures containing radioactive Pu. Unfortunately, such studies cannot be performed on large time scales as well as one cannot make any predictions for the system where many nuclear decays occur, since the microscopic level description imposes a restriction on a space scale as well. Therefore, it is necessary to develop a model allowing us to consider the system at a mesoscopic level.

In the present study, we propose a simple mesoscopic model of surface destruction processes in NFC materials, which is implemented on two-dimensional lattice with the use of a stochastic algorithm similar to the cellular automata concept [26, 27]. It is assumed that the detachment of nanoparticles at the NFC material surface results from the formation of damaged regions and microfracturing in the vicinity of the locations where nuclear decays take place. It is also assumed that the heavy nuclear recoils due to  $\alpha$ -decays are responsible for the formation of the damaged regions inside the NFC material. The technique used in the study allows us to run simulations at a mesoscopic level and to describe the surface evolution in large time scales. Thus, the characteristics such as chemical roughness, the mean-square front width and the yield of a material can be easily obtained from simulations. Our main goal is to get histograms of the particles formed during the surface destruction of NFC material. We compare the obtained histograms with the experimental results obtained for the NFC material formed in the well-known heavy nuclear accident at the Chernobyl nuclear power plant [28].

This paper is organized as follows. In section 2, we discuss the physical aspects and review some literature related to the damage and destruction processes in NFC materials. A stochastic model developed in our study is described in section 3. In section 4, we present a discussion of the obtained results. Finally, we conclude the paper in the last section.

## 2. Physical aspects

To date, many studies can be found in literature which are devoted to the study of the damage and destruction processes of the solid material surface due to *external* factors such as a high energy particle bombardment, while there is a lack of theoretical studies of the same processes for the NFC materials where the *internal* factors cause a surface destruction. However, one can notice similarities between the processes occurring near the surface in the self-irradiated material and the sputtering processes due to a surface bombardment with a flux of energetic particles. In the case of collisions between the beam and the target, one can observe a formation of cascades of atom displacements, and as a consequence, the creation of new structures and defects inside the material, which lead to a surface reconstruction and particles emission. For energetic incident beams, the sputtered particles can be large clusters of atoms. These clusters are formed in the near-surface region due to a multiple breaking of bonds [29, 30]. The magnitude of these effects specifically depends on the nature of the particles forming the beam and on their energy as well as on the nature of a target material. When a target and a beam contain the same chemical species, this process is called a self-sputtering. The self-sputtering is also widely studied for materials bombarded with projectiles of different energies [31–33] and sizes [34, 35].

In the case of sputtering phenomena as well as in the case of self-irradiated materials, we deal with energy dissipation, which leads to the formation of atomic displacement cascades [4, 30]. The main difference is that in the first case, the cascades are initiated at the surface, and the atoms or atomic clusters escape from the surface immediately. In the second case, the cascades start in the bulk. Due to  $\alpha$ -decays occurring in NFC material and a heavy nuclear recoil appears. As a consequence, an energy in the range of 40–100 keV disperses causing a local structure transformation. As a result of elastic collisions between atoms and heavy nuclei, the cascades of atomic displacements around  $\alpha$ -decay locations must occur [2, 4, 7, 36, 37]. The formation of atomic displacement cascades produced

by an elastic collision with some energetic particles was studied by molecular dynamics [7, 8, 38] and also observed from experiment [39]. The sizes of atomic collision cascades depending on the value of the particle energy estimated in these investigations are in the range of 25–30 nm. The same result was obtained by Baryakhtar et al. [28] for lava-like fuel containing materials (LFCM) formed in the Chernobyl heavy nuclear accident [40, 41]. A microscopic structure of a damaged region is disordered. At the same time, it is known that such disordered regions cause local tensions, which are responsible for the defects and microfractures formation in NFC materials [3–5, 18] and they can crucially reflect on the material durability [4, 36]. However, the fractures produced far from the material surface may not play an essential role in the material destruction due to two factors: i) because they are confined in the stable material parts; ii) they can be healed in a quite short time due to relaxation processes [42]. On the other hand, when fractures appear close to the surface, their boundaries can reach a surface and detach parts of the material. A size of a detached particle depends on geometrical sizes of the fractures which are defined by mechanical properties of the material considered as well as by the collision energy.

### 3. Modelling

#### 3.1. General concept

We propose a simple model sufficient to describe the cluster formation in terms of two parameters model. First we assume that we have a lattice with the sites from which nuclear events can be initiated. When one of the events occurs at some given site, the damage randomly expands producing defects in the vicinity of this site. For instance, a formation of a cascade of atom displacements (damaged region) takes place. In this case, one of the model parameters should relate to an area of a contact surface between the damaged region and the rest of the material forming a fracture. Another parameter corresponds to the frequency of nuclear events per volume of the NFC material, which directly depends on the concentration of nuclear fuel. A fracture can lead to the detachment of a piece of the material (particle detachment) when both two conditions are valid: i) boundaries of the fracture totally belong to the surface; ii) the fracture is open toward the surface, e.g., it should have a hemisphere-like or a cap-like shape with a basis directed toward the surface. The sequential particle detachments lead to the formation of a specific front surface which is characterized by its roughness.

To facilitate our simulations, we consider a two-dimensional model of the system presented as its projection. Therefore, the NFC material is described by its profile in  $XY$  coordinates, where the surface destruction process proceeds along  $Y$ -axis. In this case, the area of a fracture is reduced to the length of its projection, and for a particle detachment it should be of an arc-like shape. Moreover, the front surface formed during the destruction process in two dimensions reduces to a line, and hereafter we refer to it as a front line (FL).

#### 3.2. Stochastic model

A two-dimensional model is presented as a square lattice with 4 or von Neumann connectivity [43]. The simulation box is of the size of  $N_x \times N_y$  and the periodical boundary conditions are applied along  $X$ -axis. The sites of the lattice are of two types corresponding to two kinds of species. The first kind of sites represents the regions of pristine solid material and the second type represents the regions containing nuclear fuel inclusions, which correspond to impact centers (ICs) where the damage processes can start from. We reduce the number of characteristic lengths of the system to only one — the lattice constant,  $a$ , and it is subsequently our unit of length. The IC sites are located randomly on the lattice. We denote their concentration or number density as  $f_a$ . Each of the IC sites is chosen randomly to build paths of a fracture initiated from this IC (OA and OB in figure 1). Within the model proposed, the fracture is built by two different paths, which evolve in opposite directions. Such a fracture formation can potentially lead to a detachment of a piece of material surface. In this case, two possibilities to start the fracture creation are considered: OA is directed to the left from the chosen IC site while OB goes to the right, or OA goes up while OB goes down. The paths of fracture propagation is modelled as a random walk. Due to the assumption of a limited length of the fracture that can be formed in the material, the number of steps of

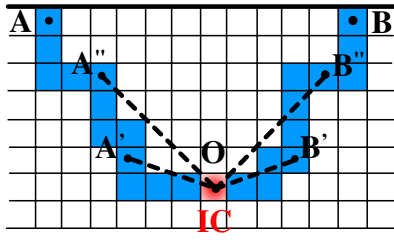


**Figure 1.** (Color online) Example of fracture propagation. Filled blue cells denote random walk paths to build a fracture. The central red cell (site “O”) corresponds to the impact center (IC).

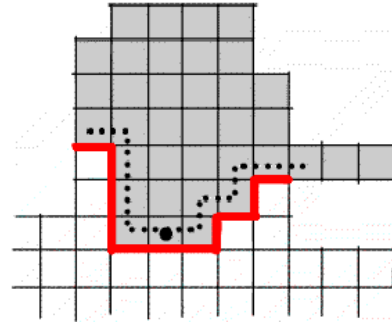


**Figure 2.** (Color online) Cluster detachment for  $N_{\text{srw}} = 6$ . Filled grey cells belong to the particle to be detached. The dotted lines denote random walk paths initiated from the IC site (big point) and the thick red line denotes the corresponding fracture.

a random walk cannot exceed the specified parameter  $N_{\text{srw}}$ , which is equal to a half the maximum length of fractures. Another restriction introduced in the model requires that the distances between the ends of the fracture and its initial point should increase during its propagation as shown in figure 1:  $OA'' > OA'$  and  $OB'' > OB'$ . This condition prevents the self-crossing of the fracture. In this way, the ends of a fracture propagate away one from another forming an arc-like fracture. It is quite reasonable to give some preferable direction for the fracture propagation dependent on a deformation geometry around the IC considered (especially when the maximum length of a fracture is rather small). If both ends of the fracture reach the surface, then the constructed fracture leads to a detachment of the material cluster (figure 2). Otherwise, the event is discarded, i.e., when the fracture paths stop somewhere in the bulk. In this case, we forget about it supposing that the relaxation processes are fast enough for the fracture to be healed [42]. To obtain the results with a sufficient accuracy for the surface roughness for each pair of the parameters  $N_{\text{srw}}$  and  $f_d$ , we perform an average over 30 independent simulation runs. Each simulation run takes 200000 steps. One simulation step corresponds to one particle detachment. The size of a lattice taken of  $N_x = 1000$  and  $N_y = 1000$  is found to be sufficient to minimize the boundary condition effects and to consider rather large FL widths. The events for the size histogram are collected in a stationary regime of the material destruction after 50000 simulation steps. To identify the clusters of sites formed during particle detachments the Hoshen-Kopelman algorithm is used [44].

## 4. Results and discussion

To describe the properties of the front line (FL) we introduce standard functions, which characterize the growth processes [45]. First we consider the roughness of the FL as a function of the number of simulation time steps  $N_{\text{steps}}$  for different values of the parameters  $f_d$  and  $N_{\text{srw}}$ . The roughness is given by the factor defined as a ratio of the number of sites  $N_s$  in the FL to the initial number  $N_x$  of sites in the smooth surface  $N_x = 1000$ . After  $N_{\text{step}}$ , the roughness factor is given by

$$r(N_{\text{steps}}) = \frac{N_s(N_{\text{steps}})}{N_x}. \quad (4.1)$$

We may notice that according to our algorithm, the  $N_s$  sites are only formed by the host material (free of any nuclear fuel inclusions). Thus, there is no IC site on the surface, by construction. For the initial FL there is no roughness, i.e.,  $r(0) = 1$ . After some simulation steps, we observe an increase of the roughness factor, due to the particle detachment process (figure 3). After 50000 simulation steps we get a stationary regime characterized by a constant value  $r$  for all the parameters considered in our study. In figure 4 we plot  $r$  as a function of  $f_d$  and for two values of  $N_{\text{srw}}$ . We also observe that  $r$  increases when the density of ICs decreases and about  $f_d = 0.80$  the roughness becomes almost independent of  $N_{\text{srw}}$ . We expect that this weakening related to the average distance between ICs becomes less than the

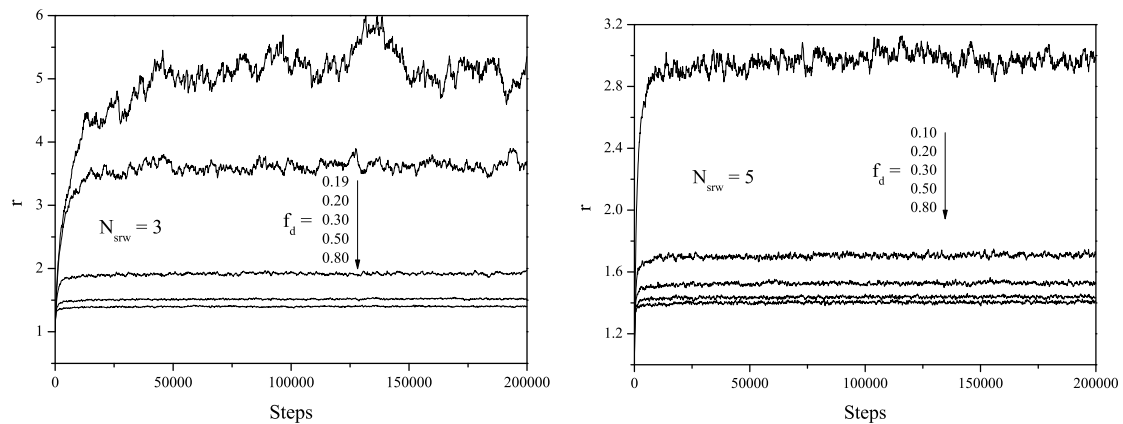


**Figure 3.** Variation of the ratio  $r$  versus a number of simulation steps obtained for  $N_{\text{srw}} = 3$  and  $N_{\text{srw}} = 5$ , and for the different density  $f_d$ .

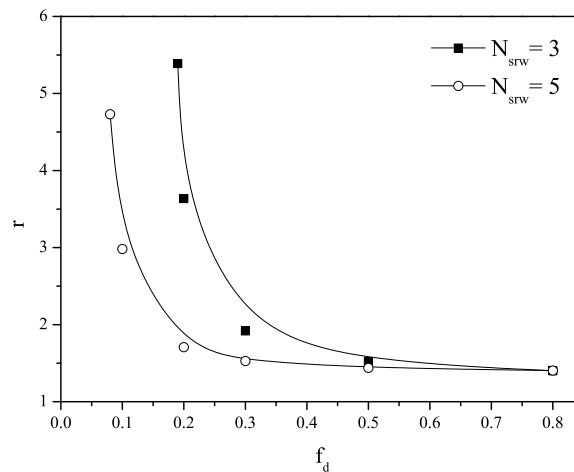


**Figure 4.** The dependence of roughness  $r$  on the  $f_d$  for  $N_{\text{srw}} = 3$  (square symbols) and  $N_{\text{srw}} = 5$  (circle symbols).

mean length of a fracture. This can be also explained by the fact that the mean size of detached particles increases monotonously when we decrease  $f_d$  (table 1). It is also worth noting that there exists a critical value  $f_c$  such that for  $f_d < f_c$  the destruction process stops. This is related to the distances between ICs, which are too large in order to provide continuous detachments of particles, and at some step one quickly faces a situation when  $N_{\text{srw}}$  is not sufficient to build a path from any IC in the system to the surface. For  $N_{\text{srw}} = 3$  we obtain  $f_c$  about 0.19, and for  $N_{\text{srw}} = 5$ , the critical density  $f_c$  is found at lower values of  $f_d$  which are near 0.08. One can observe in figure 4 that in the vicinity of  $f_c$ , the roughness  $r$  increases drastically, and since the critical density  $f_c$  is higher for smaller  $N_{\text{srw}}$ , the roughness increases faster with a decrease of  $f_d$ . Therefore, we always obtain larger values of the roughness for smaller  $N_{\text{srw}}$ . This looks surprising because one would expect a larger roughness in the case corresponding to a larger particles detachment. This is certainly true if a single particle detachment at a flat surface is considered. However, we have a series of detachments leading to a formation of a complex rough surface. It is really difficult to predict for which exactly  $N_{\text{srw}}$ , the roughness is higher without doing simulation. Moreover, it should be noted that  $N_{\text{srw}}$  is just the maximum length of a fracture, and it means that actual lengths of fractures causing particle detachments can be smaller than the given  $N_{\text{srw}}$ . Therefore, one can expect a distribution of lengths of such fractures. At the same time, the roughness results from the averaging along FL and

**Table 1.** The mean sizes of particles for the given parameters.

$f_d$	$N_{srw} = 3$	$N_{srw} = 5$
0.10	–	14.78
0.20	10.06	<b>13.58</b>
0.30	<b>9.72</b>	<b>12.49</b>
0.50	<b>8.60</b>	<b>11.70</b>
0.80	<b>8.05</b>	<b>11.32</b>

the real contribution of fractures of different sizes to the total surface formation is unclear. On the other hand, the behaviour of the roughness at different  $N_{srw}$  can be explained by that for a larger  $N_{srw}$  where the destruction process proceeds more intensively than for smaller  $N_{srw}$ , and this leads to a better smoothing of FL.

A constant value for the roughness factor  $r$  means that the length of the FL is constant but nevertheless different shapes can be observed for the FL. The deformations at a constant length can be visualized with a flexible cord rearranged without stretching or squeezing. Therefore, the roughness factor  $r$  does not reflect all the geometrical features of the FL. Another parameter associated with the roughness is the width of the FL defined as the root of mean-square deviation  $\sigma$  of the FL from its mean position [45]:

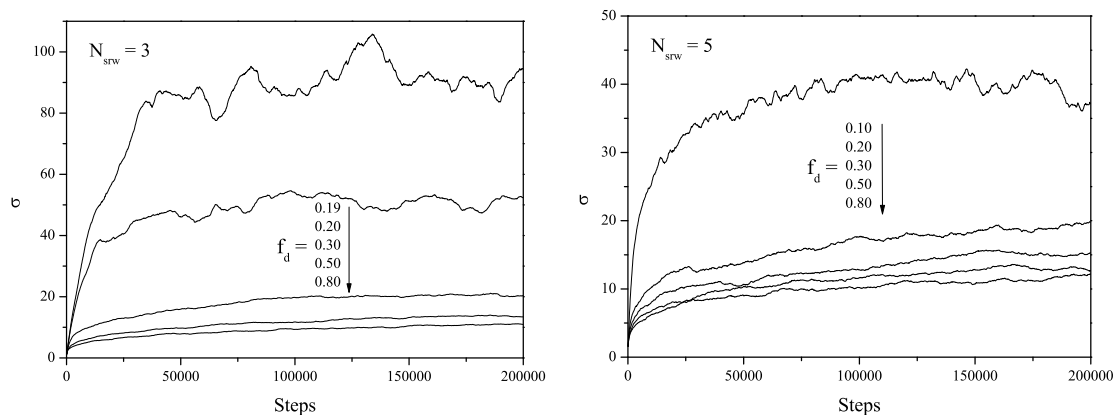
$$\sigma(N_{steps}) = \left\{ \frac{1}{N_x} \sum_{i=1}^{N_x} [h_i - h(N_{steps})]^2 \right\}^{1/2}, \quad (4.2)$$

where  $h_i$  is the height of the pile of material sites in the  $i$ -th column from the bottom of the simulation box up to the first environment site in this column. The mean position of the FL is defined as usual [45]:

$$h(N_{steps}) = \frac{1}{N_x} \sum_{i=1}^{N_x} h_i. \quad (4.3)$$

The dependence of  $\sigma(N_{steps})$  on the number of simulation steps is shown in figure 5. As expected, the average width of the front profile increases when the density of ICs in the system decreases. Qualitatively, the evolution of  $\sigma$  is similar to that of  $r$ , but the convergence to the stationary regime is noticeably slower.

The time evolution of the mean position of the FL calculated from the expression (4.3) gives an estimation of degradation rate for the material. In our algorithm, one detachment of the particle occurs

**Figure 5.** The evolution of the front width as given by the root of mean-square deviation from the mean position. The parameters are the same as in figure 3.

per one simulation step. The simulation step can be related to real time if we know the so-called dust productivity parameter which is known in some experiments. Unfortunately, we have no such parameter in the case of the LFCM. Therefore, we limit the analysis of the FL to its dependence on the number of simulation steps. We observe the existence of a stationary regime for the displacement of the FL. After a large number of simulation steps, the mean position of FL is given by  $pN_{\text{step}}$  and the slopes  $p$  have been estimated (table 2). It is observed that the lower is the value of  $f_d$  the larger is the slope. Due to a single particle detachment per a simulation step, the higher slopes indicate that the larger sizes of particles are detached. As shown above, the lower is  $f_d$  the higher is the roughness and the larger are the sizes of the particles emitted. Therefore, the results presented in table 2 are consistent with that in table 1. Indeed, they are in a very good agreement for the values of  $f_d$  higher than 0.30 and  $N_{\text{srw}} = 3$  as well as for

**Table 2.** The slopes of the dependencies of the mean position of FL for the same parameters as in table 1.

$f_d$	$N_{\text{srw}} = 3$	$N_{\text{srw}} = 5$
	$\times 10^{-3}$	$\times 10^{-3}$
0.10	–	19.12
0.20	13.24	<b>13.74</b>
0.30	<b>9.92</b>	<b>12.51</b>
0.50	<b>8.60</b>	<b>11.70</b>
0.80	<b>8.05</b>	<b>11.32</b>

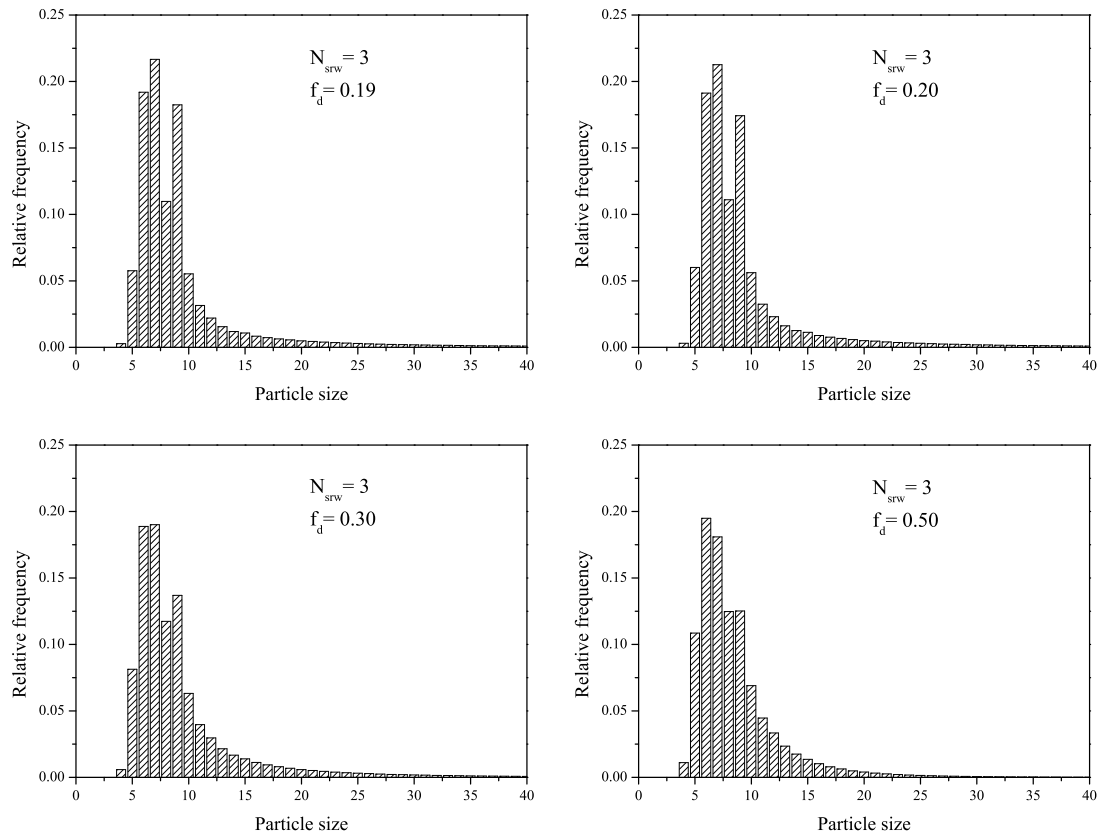


**Figure 6.** The distributions of the emitted particles for  $N_{\text{srw}} = 3$  and different densities  $f_d$ .

$f_d$  higher than 0.20 and  $N_{srw} = 5$  (marked bold). Near the critical values of ICs density,  $f_c$ , there is a difference observed between these two cases.

The events for the size histogram are collected in a stationary regime of the material destruction after 50000 simulation steps. From the simulations we can calculate the total number of the emitted particles and estimate the relative frequency of a given particle size. By such procedure, the histogram is normalized and from this histogram we may determine the mean size of the emitted particles (table 1). In figures 6 and 7 we present the calculated histograms. One can see that the dispersion of the particle sizes is not essentially affected by the IC density while the mean size of the detached particles depends on  $f_d$  as it is shown in table 1. At low  $f_d$ , there are two sharp peaks on the histograms (figure 6). When  $f_d$  increases, the second peak is suppressed and the histogram becomes smoother. At a sufficiently high density ( $f_d = 0.50$ ), the second peak disappears completely. Simultaneously, the first peak shifts to smaller sizes. The dispersion of the size distribution is strongly affected by the  $N_{srw}$  parameter. In figure 7, the histograms for the cases of  $N_{srw} = 2$  and  $N_{srw} = 5$  at  $f_d = 0.50$  are presented. For  $N_{srw} = 2$ , the dispersion of particle sizes is much smaller than for  $N_{srw} = 5$ . Hence, for longer fractures we may obtain larger particles.

The projected histogram calculated for  $f_d = 0.19-0.3$  and  $N_{srw} = 3$  (figure 6) is in a remarkable qualitative agreement with that shown in figure 8 for the data of Baryakhtar *et al.* [28]. Herein above we have given the relation between the effective radius, the mean number of sites and the lattice constant  $a$ . If

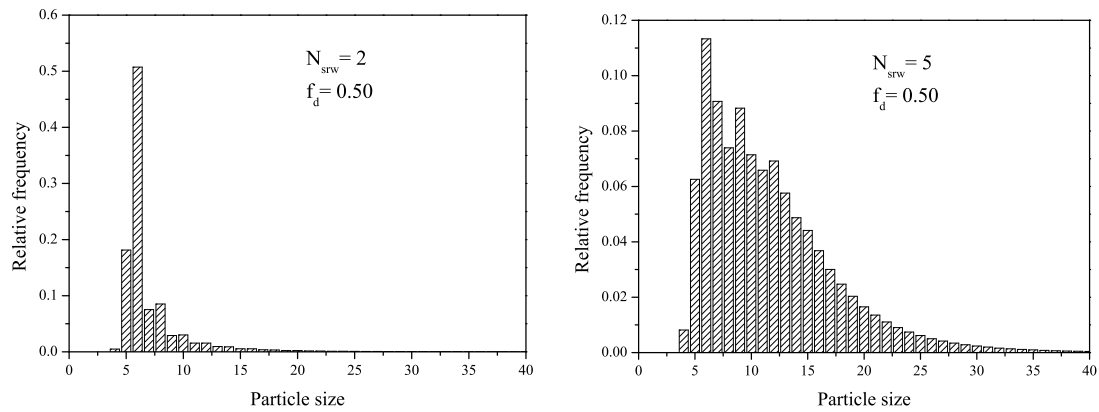


**Figure 7.** The distributions of the emitted particles for  $N_{srw} = 2$  and  $N_{srw} = 5$  at the density  $f_d=0.50$ .

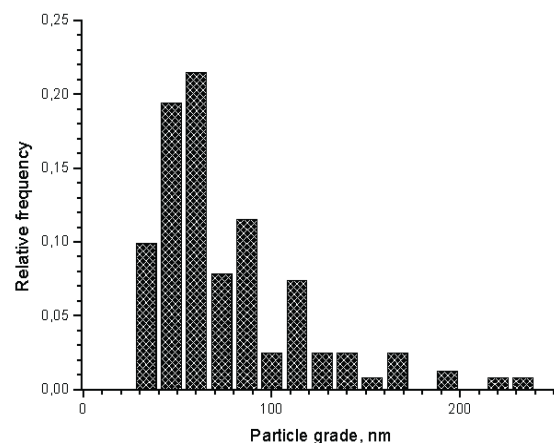


**Figure 8.** The distribution of the emitted particles obtained from the experiment for the material containing a lava-like nuclear fuel by Baryakhtar *et al.* [28].



we fit the effective radius to the value  $R_{\max}$  associated with the maximum of the experimental histogram and if for the number of sites we take its value  $n_{\max}$  obtained from the calculated histogram, we can get an estimation of the lattice constant as

$$a \approx R_{\max} \sqrt{\pi/n_{\max}} = 20.1 \text{ nm}, \quad (4.4)$$

where  $R_{\max} = D/2$ , while  $D = 60 \text{ nm}$  is the diameter of the particles at the first maximum in figure 8, and  $n_{\max} = 7$  is the corresponding size of the particles in terms of a number of sites obtained from the simulation. The calculated value of  $a$  has the same order of magnitude as the damaged regions 25–30 nm observed in [28] and related to a size of the elementary cluster that can be detached. The value of the parameter  $N_{\text{srw}}$  giving the maximum length of the fracture can be derived as  $l = La = (2N_{\text{srw}} + 1)a \sim 141 \text{ nm}$  for  $N_{\text{srw}} = 3$ . The value of  $l$  is far lower than the critical one when the fracture starts to propagate continuously [46]. Due to this, the immediate destruction of the material only appears in its subsurface region or when fractures form an infinite network inside the material bulk. In the given study, we consider the first case. As it is shown above, the surface roughness keeps constant during this process. For a more thorough verification of the model, a comparison of the experimentally determined and simulated surface roughness can be useful. Such results would allow us to adjust the model parameters so far undetermined in the absence of the experimental data.

## 5. Conclusions

We propose a stochastic model to simulate the destruction processes in nuclear fuel containing (NFC) materials. In this study, we focus on the surface erosion processes leading to the emission of material particles. It is assumed that the erosion of the NFC material surface results from numerous  $\alpha$ -decay events in the subsurface region, which are accompanied with heavy nuclear recoils producing damages in the material. The approach used in the study allows us to run simulations at the mesoscopic level and to describe the surface evolution in large time scales. A quantitative description of this model is presented as its projection on a two-dimensional lattice.

The model is defined by two parameters, one of which is related to the number density of the nuclear fuel in the material, and another characterizes a maximum size of the defects (fractures) produced by heavy nuclear recoils. Different pairs of these parameters have been checked and the corresponding characteristics, such as surface roughness, mean-square width of the front and the yield of material are calculated. These results were obtained in a stationary regime of the NFC material destruction process. However, it should be noted that the stationary regime can be achieved only when the number density  $f_d$  and the maximum length of fractures  $2N_{\text{srw}}$  are large enough. For instance, for each value of the parameter  $N_{\text{srw}}$ , one can find a critical concentration  $f_c$  below which the destruction process cannot proceed. On the contrary, for  $f_d$  higher than  $f_c$ , we find at longer times a stationary regime. It is observed that for high values of  $f_d$ , the roughness of NFC material surface is rather small. However, a decrease of  $f_d$  leads to an increase of the roughness as well as of the mean-square width of the front and the mean particle size. Moreover, it is noticed that the maximum values of these characteristics are reached if  $f_d$  tends to  $f_c$ .

The size histograms of the particles produced during the erosion of the material surface are built during simulations. These distributions are characterized by different dispersions and mean values of the particle sizes depending on  $f_d$  and  $N_{\text{srw}}$  chosen. It is shown that our theoretical predictions are in a good agreement with the experimental histograms of particle sizes obtained due to destruction processes of the material containing lava-like nuclear fuel formed during the Chernobyl catastrophe [28]. We have also checked that the parameters of the model in this case are of a correct order of magnitude.

## Acknowledgement

The simulations have been done on the computing cluster of the Institute for Condensed Matter Physics (Lviv, Ukraine).

## References

1. Matzke HJ., *Radiat. Eff. Defects Solids*, 1982, **64**, 3, doi:10.1080/00337578208222984.
2. Weber W.J., *J. Mater. Res.*, 1990, **5**, 2687, doi:10.1557/JMR.1990.2687.
3. Weber W.J., Ewing R.C., Catlow C.R.A., Diaz de la Rubia T., Hobbs L.W., Kinoshita C., Matzke HJ., Motta A.T., Nastasi M., Salje E.K.H., Vance E.R., Zinkle S.J., *J. Mater. Res.*, 1998, **13**, No. 6, 1434–1484, doi:10.1557/JMR.1998.0205.
4. Ewing R.C., Weber W.J., Clinard F.W. (Jr.), *Prog. Nucl. Energy*, 1995, **29**, 63, doi:10.1016/0149-1970(94)00016-Y.
5. Evron R., Kimmel G., Eyal Y., *J. Nucl. Mater.*, 1994, **217**, 54–66, doi:10.1016/0022-3115(94)90304-2.
6. Fayek M., Anovitz L.M., Cole D.R., Bostick D.A., *Geochim. Cosmochim. Acta*, 2011, **75**, 3677–3686, doi:10.1016/j.gca.2011.03.040.
7. Trachenko K., Dove M.T., Salje E.K.H., *J. Phys.: Condens. Matter*, 2001, **13**, 1947, doi:10.1088/0953-8984/13/9/317.
8. Trachenko K., Dove M.T., Artacho E., Todorov I.T., Smith W., *Phys. Rev. B*, 2006, **73**, 174207, doi:10.1103/PhysRevB.73.174207.
9. Trachenko K., Zarkadoula E., Todorov I.T., Dove M.T., Dunstan D.J., Nordlund K., *Nucl. Instrum. Methods Phys. Res., Sect. B*, 2012, **277**, 6–13, doi:10.1016/j.nimb.2011.12.058.
10. Bishop C.L., Grimes R.W., Parfitt D.C., *Nucl. Instrum. Methods Phys. Res., Sect. B*, 2010, **268**, 2915–2917, doi:10.1016/j.nimb.2010.05.007.
11. Van Brutzel L., Rarivomanantsoa M., Ghaleb D., *J. Nucl. Mater.*, 2006, **354**, 28–35, doi:10.1016/j.jnucmat.2006.01.020.
12. Van Brutzel L., Vincent-Aublant E., Delaye J.-M., *Nucl. Instrum. Methods Phys. Res., Sect. B*, 2009, **267**, 3013–3016, doi:10.1016/j.nimb.2009.06.078.
13. Martin G., Maillard S., Van Brutzel L., Garcia P., Dorado B., Valot C., *J. Nucl. Mater.*, 2009, **385**, 351–357, doi:10.1016/j.jnucmat.2008.12.010.
14. Martin G., Garcia P., Van Brutzel L., Dorado B., Maillard S., *Nucl. Instrum. Methods Phys. Res., Sect. B*, 2011, **269**, 1727–1730, doi:10.1016/j.nimb.2010.12.075.
15. Tian X.F., Gao T., Long C., Li J.K., Jiang G., Xiao H., *Nucl. Instrum. Methods Phys. Res., Sect. B*, 2011, **269**, 1771–1776, doi:10.1016/j.nimb.2011.04.115.
16. Delaye J.M., Peugeot S., Bureau G., Calas G., *J. Non-Cryst. Solids*, 2011, **357**, 2763–2768, doi:10.1016/j.jnoncrysol.2011.02.026.
17. Dewan L., Hobbs L.W., Delaye J.M., *J. Non-Cryst. Solids*, 2012, **358**, 3427–3432, doi:10.1016/j.jnoncrysol.2012.04.033.
18. Kieu L.H., Delaye J.M., Stolz C., *J. Non-Cryst. Solids*, 2012, **358**, 3268–3279, doi:10.1016/j.jnoncrysol.2012.07.037.
19. Devanathan R., Corrales L.R., Weber W.J., Chartier A., Meis C., *Nucl. Instrum. Methods Phys. Res., Sect. B*, 2005, **228**, 299–303, doi:10.1016/j.nimb.2004.10.060.
20. Heinisch H.L., Weber W.J., *Nucl. Instrum. Methods Phys. Res., Sect. B*, 2005, **228**, 293–298, doi:10.1016/j.nimb.2004.10.059.
21. Chung B.W., Thompson S.R., Lema K.E., Hiromoto D.S., Ebbinghaus B.B., *J. Nucl. Mater.*, 2009, **385**, 91–94, doi:10.1016/j.jnucmat.2008.09.031.
22. Baclet N., Oudot B., Grynszpan R., Jolly L., Ravat B., Faure P., Berlu L., Jomard G., *J. Alloys Compd.*, 2007, **444–445**, 305–309, doi:10.1016/j.jallcom.2006.10.156.
23. Dremov V.V., Sapozhnikov F.A., Samarin S.I., Modestov D.G., Chizhkova N.E., *J. Alloys Compd.*, 2007, **444–445**, 197–201, doi:10.1016/j.jallcom.2006.10.003.
24. Robinson M., Kenny S.D., Smith R., Storr M.T., McGee E., *Nucl. Instrum. Methods Phys. Res., Sect. B*, 2009, **267**, 2967–2970, doi:10.1016/j.nimb.2009.06.113.
25. Geisler T., Trachenko K., Ríos S., Dove M.T., Salje E.K.H., *J. Phys.: Condens. Matter*, 2003, **15**, L597–L605, doi:10.1088/0953-8984/15/37/L07.
26. Taleb A., Stafiej J., Chaussé A., Messina R., Badiali J.P., *J. Electroanal. Chem.*, 2001, **500**, 554, doi:10.1016/S0022-0728(00)00433-2.
27. Patsahan T., Taleb A., Stafiej J., Badiali J.P., *Condens. Matter Phys.*, 2007, **10**, 579–585, doi:10.5488/CMP.10.4.579.
28. Baryakhtar V., Gonchar V., Zhidkov A., Zhydkov V., *Condens. Matter Phys.*, 2002, **5**, 449, doi:10.5488/CMP.5.3.449.
29. Wucher A., Garrison B.J., *J. Chem. Phys.*, 1996, **105**, 5999, doi:10.1063/1.472451.
30. Betz G., Husinsky W., *Philos. Trans. R. Soc. London, Ser. A*, 2004, **362**, 177, doi:10.1098/rsta.2003.1302.

31. Robinson M.T., J. Appl. Phys., 1983, **54**, 2650, doi:10.1063/1.332267.
32. Voskoboinikov R.E., Osetsky Yu.N., Bacon D.J., Nucl. Instrum. Methods Phys. Res., Sect. B, 2006, **242**, 68–70, doi:10.1016/j.nimb.2005.08.166.
33. Salonen E., Nordlund K., Keinonen J., Wu C.H., J. Nucl. Mater., 2003, **313–316**, 404, doi:10.1016/S0022-3115(02)01397-1.
34. Li A., Watts R.O., J. Chem. Phys., 1995, **103**, 7187, doi:10.1063/1.470347.
35. Lindenblatt M., Heinrich R., Wucher A., Garrison B.J., J. Chem. Phys., 2001, **115**, 8643, doi:10.1063/1.1404982.
36. Day D.H., Hughes A.E., Leake J.W., Marples J.A.C., Marsh G.P., Rae J., Wade B.O., Rep. Prog. Phys., 1985, **48**, 101, doi:10.1088/0034-4885/48/1/003.
37. Palenik C.S., Nasdala L., Ewing R.C., Am. Mineral., 2003, **88**, 770–781, doi:10.2138/am-2003-5-606.
38. Kubota A., Caturla M.J., Payne S.A., Diaz de la Rubia T., Latkowski J.F., J. Nucl. Mater., 2002, **307–311**, 891, doi:10.1016/S0022-3115(02)01008-5.
39. Kubota A., Caturla M.J., Stolken J., Sadigh B., Reyes S., Diaz de la Rubia T., Latkowski J.F., Nucl. Instrum. Methods Phys. Res., Sect. B, 2003, **202**, 88, doi:10.1016/S0168-583X(02)01837-2.
40. Pazukhin E.M., Radiochemistry, 1994, **36**, 97.
41. Zhidkov A.V., Problems of Chornobyl, 2001, **7**, 23.
42. Wronkiewicz D.J., Preprint ANL/CMT/CP–80028, Argonne National Laboratory, 1993.
43. Chopard B., Droz M., Cellular Automata Modeling of Physical Systems, Cambridge University Press, Cambridge, 1998.
44. Hoshen J., Kopelman R., Phys. Rev. B, 1976, **14**, 3438, doi:10.1103/PhysRevB.14.3438.
45. Barabasi A.L., Stanley H.E., Fractal Concepts in Surface Growth, Cambridge University Press, Cambridge, 1995.
46. Stashchuk M.H., Stashchuk A.M., Mater. Sci., 1998, **34**, 383, doi:10.1007/BF02355628.

## Стохастичне комп'ютерне моделювання процесів руйнування в самопроміненних матеріалах

Т. Пацаган<sup>1</sup>, А. Талеб<sup>2,3</sup>, Я. Стафієй<sup>4</sup>, М. Головко<sup>1</sup>, Ж.П. Бадіалі<sup>1,3</sup>

<sup>1</sup> Інститут фізики конденсованих систем Національної академії наук України, вул. Свенціцького, 1, 79011 Львів, Україна

<sup>2</sup> Дослідницький університет науки та літератури Парижу, Chimie ParisTech — CNRS, Інститут хімічних досліджень Парижу, Париж, Франція

<sup>3</sup> Університет П'єра і Марії Кюрі, Париж, 75231, Франція

<sup>4</sup> Університет кардинала Стефана Вишинського, факультет математики і природничих наук, Варшава, Польща

Самопромінення, що виникає внаслідок процесів поділу радіоактивних елементів, є звичним явищем, яке спостерігається в радіоактивних паливовмісних матеріалах (ПВМ). Численні  $\alpha$ -розпади призводять до перетворення локальної структури ПВМ. Ушкодження, які виникають за рахунок ударів віддачі осколків поділу важких ядер в приповерхневому шарі, можуть спричинювати відокремлення частинок матеріалу. Така поведінка є подібною до процесу розпилення, яке спостерігається під час бомбардування поверхні матеріалу потоком енергетичних частинок. Проте, в ПВМ удари ініціюються в об'ємі матеріалу. В цій роботі ми пропонуємо двовимірну мезоскопічну модель, з метою здійснення стохастичного комп'ютерного моделювання процесів руйнування, що виникають в приповерхневій області ПВМ. Ми описуємо ерозію поверхні матеріалу, зміну її шорсткості з часом і передбачаємо відокремлення частинок матеріалу. У цьому дослідженні отримано розподіли розмірів відокремлених частинок. Результати комп'ютерного моделювання якісно узгоджуються із гістограмами розмірів розпилених частинок спостережених в лаво-подібних паливовмісних масах, які сформувалися під час Чорнобильської катастрофи.

**Ключові слова:** радіоактивні паливовмісні матеріали, самопромінююче ушкодження, руйнування, шорсткість, стохастичне комп'ютерне моделювання, процес розпилення

---

---